

# Overview of **Experimental Studies** on **Inter-ELM Pedestal localized Fluctuations** and **Challenges for their Modeling**

**F. M. Laggner**<sup>1</sup>, A. Diallo<sup>2</sup>, E. Wolfrum<sup>3</sup>, M. Cavedon<sup>3</sup>, B. Vanovac<sup>3</sup>, E. Kolemen<sup>1</sup>

with contributions of

the ASDEX Upgrade Team, the DIII-D team and the EUROfusion MST1 Team

<sup>1</sup>Department of Mechanical and Aerospace Engineering, Princeton University, Princeton, New Jersey, USA

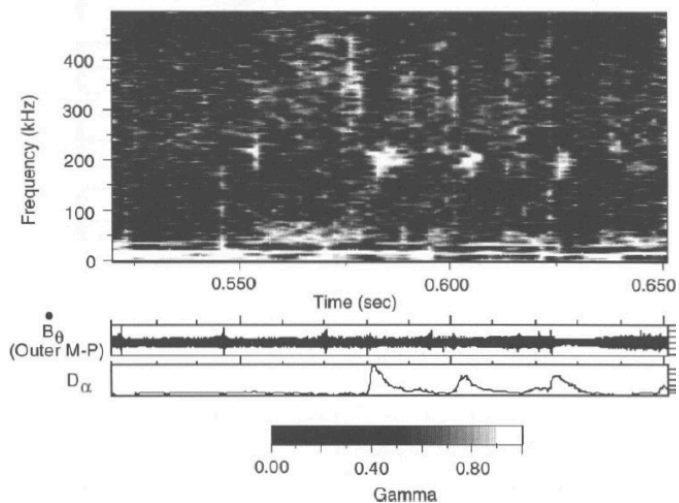
<sup>2</sup>Princeton Plasma Physics Laboratory, Princeton, New Jersey, USA

<sup>3</sup>Max-Planck-Institut für Plasmaphysik, Boltzmannstr. 2, 85748 Garching, Germany

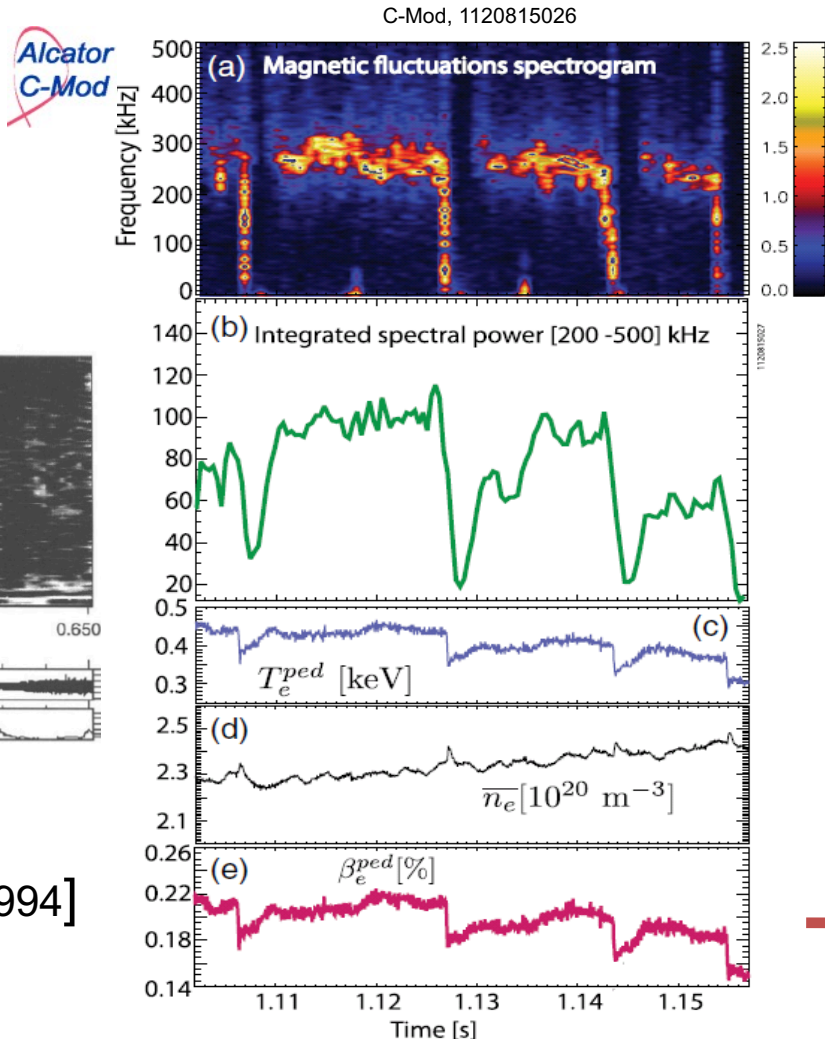
# Long effort to characterize pedestal instabilities...

JET

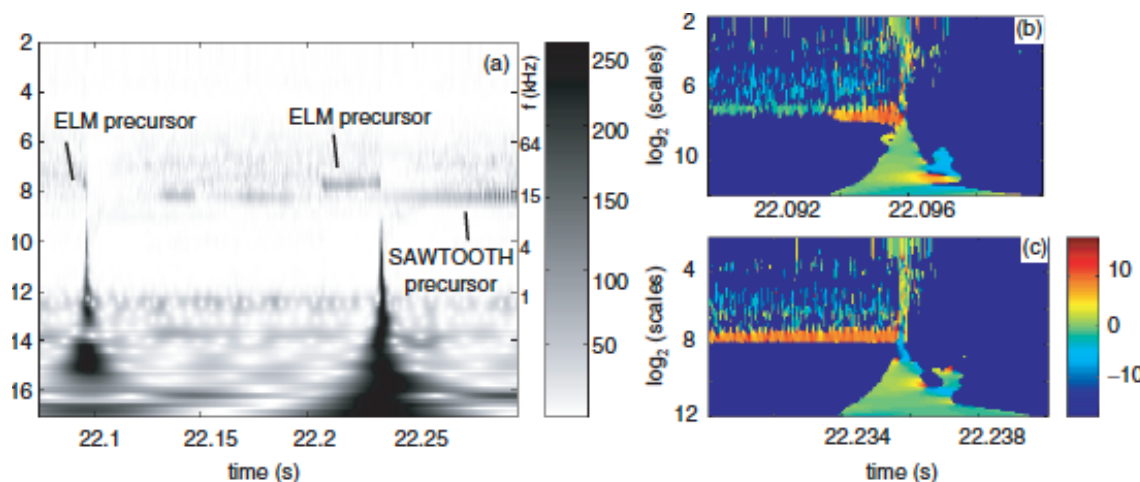
PBX-M



[S. M. Kaye et al., PPCF 1994]



[A. Diallo, et al., PRL 2014]

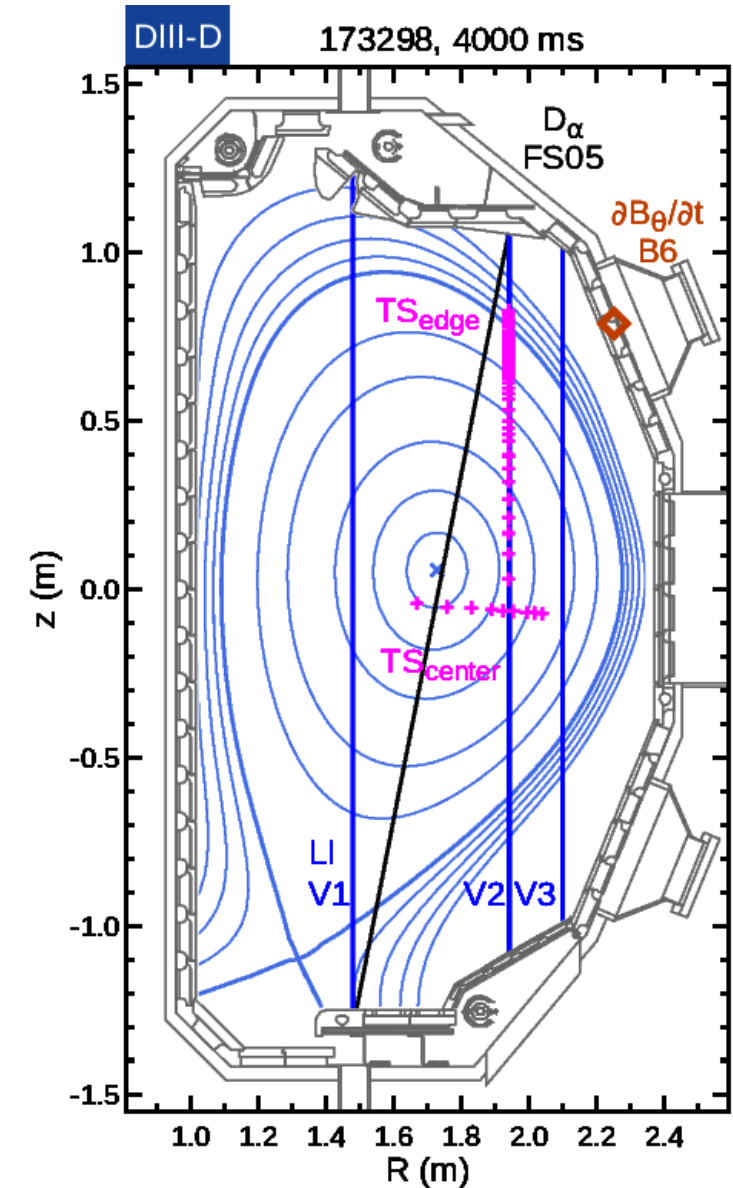
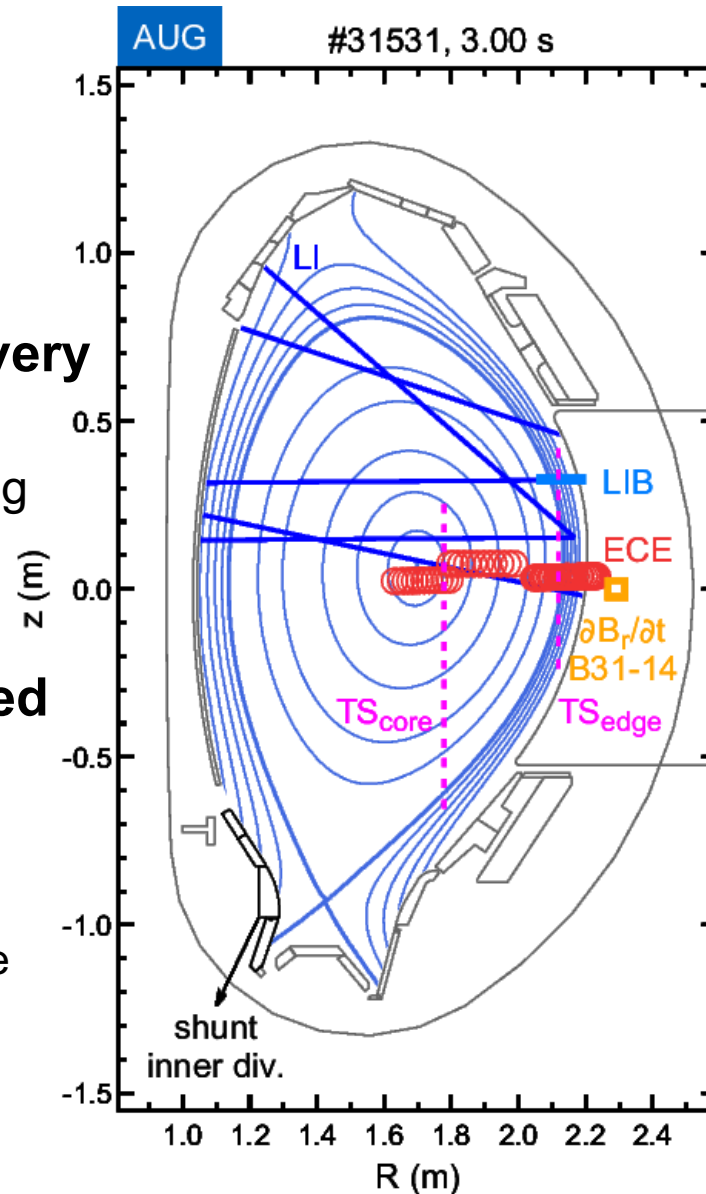


[F. M. Poli et al., PPCF 2008]

➔ Now is the time to achieve fundamental understanding of them using sophisticated modelling

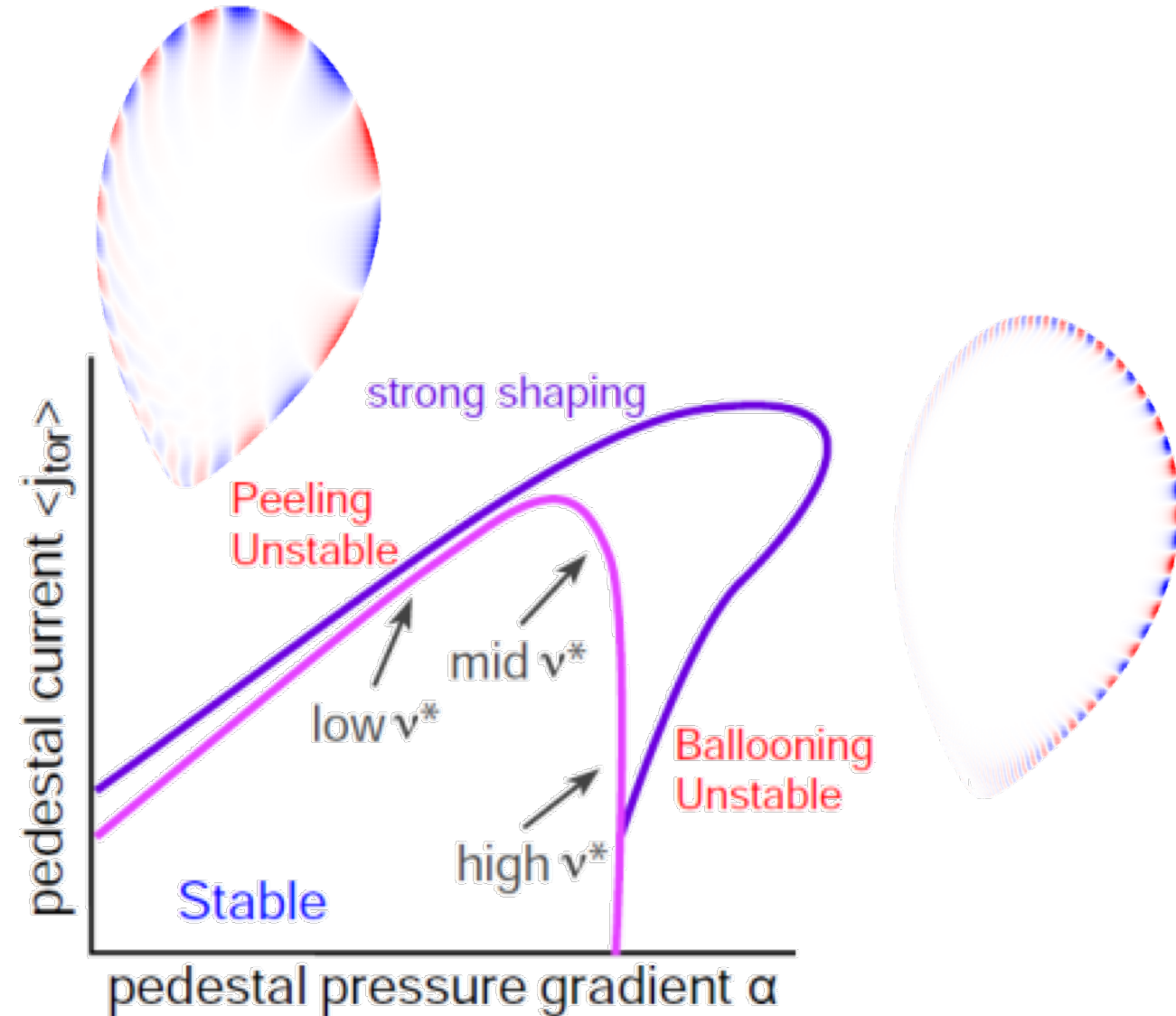
# Challenge - Diagnosing the pedestal

- **Profiles & fluctuations required for good interpretation**
- **Uncertainties are associated with every measurement**
  - Awareness necessary when interpreting
- **Understand and to consider the fundamental limitations of the utilized diagnostics**
  - Some examples:
    - ECE: shine through
    - BES: radial widening of emission profile
    - CER: assumption of equilibrium temperature



# Theory - pedestal stability

- **Peeling-ballooning P-B theory:**
  - Peeling Mode
    - Current driven instability
  - Ballooning Mode
    - Pressure driven instability
  
- **P-B gives a 'hard' limit for the edge pressure**



[P. B. Snyder et al., POP 2009]

# Theory - pedestal evolution

- **Model for ELM cycle**

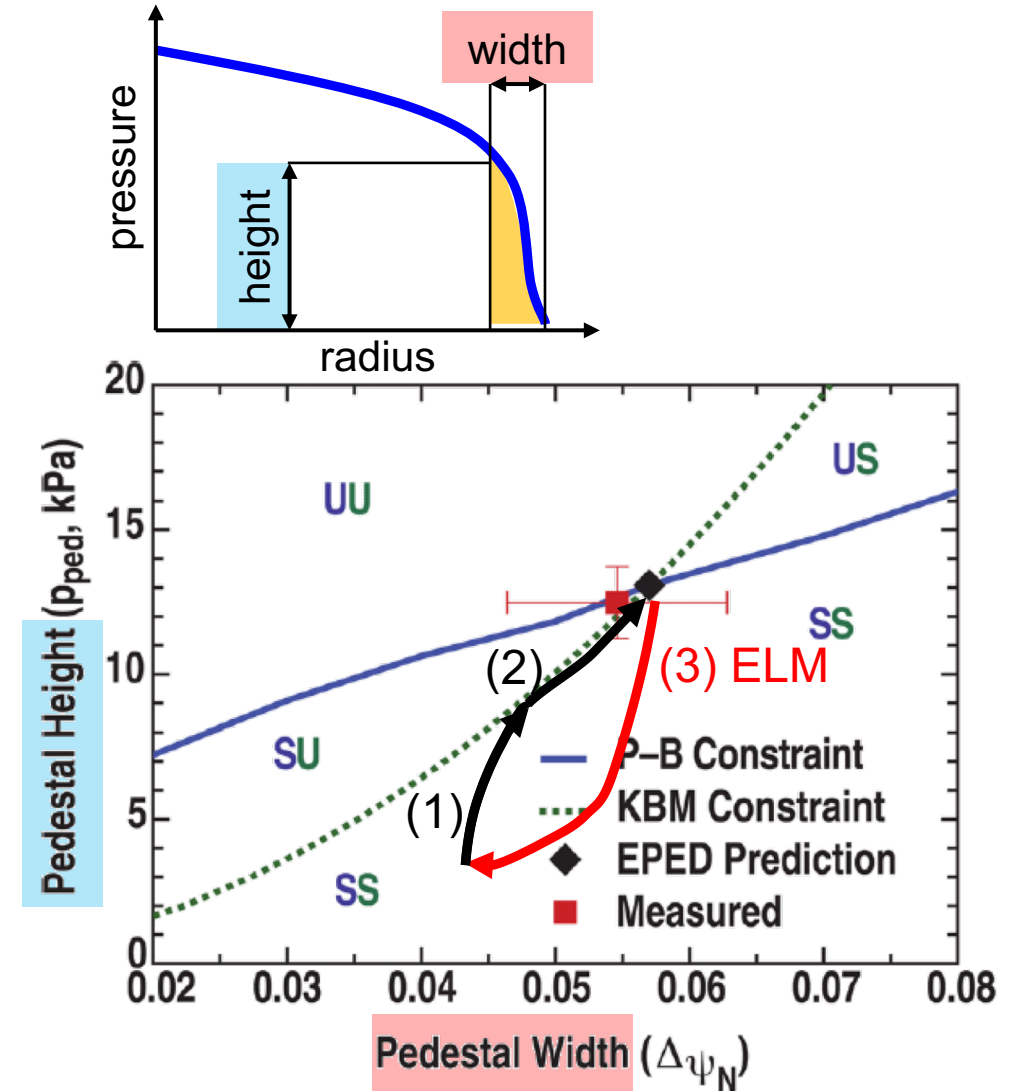
- (1) Pedestal height and width increase till kinetic ballooning mode (KBM) boundary ('soft limit') is reached
- (2) Pedestal gradient is clamped and height and width evolve along the KBM limit
- (3) ELM crash when P-B ('hard') limit is reached

- **Limitation of pedestal evolution ('soft limit') observed in several experiments**

[A. Burckhart et al., PPCF 2010]

[D. Dickinson et al., PRL 2012]

[A. Diallo et al., PRL 2014]



[P. B. Snyder et al., POP 2012]

# Drive and suppression of pedestal instabilities

- **Pressure gradient ( $\nabla p$ )**
  - Typically drives ballooning-type instabilities
    - $\nabla p$  linked to density ( $n$ ) and temperature

- **Edge current density ( $j_{\text{tor}}$ )**

- Main contribution is bootstrap current ( $j_{\text{BS}}$ )

$$j_{\text{BS}} \propto \sqrt{\varepsilon} \frac{\nabla p}{\beta_g}$$

➢ Order:  $\nabla n \sim 0.5$ ,  $\nabla T_e \sim 0.15$  and  $\nabla T_i \sim 0.1$

- Modifies the safety factor profile ( $q$ )

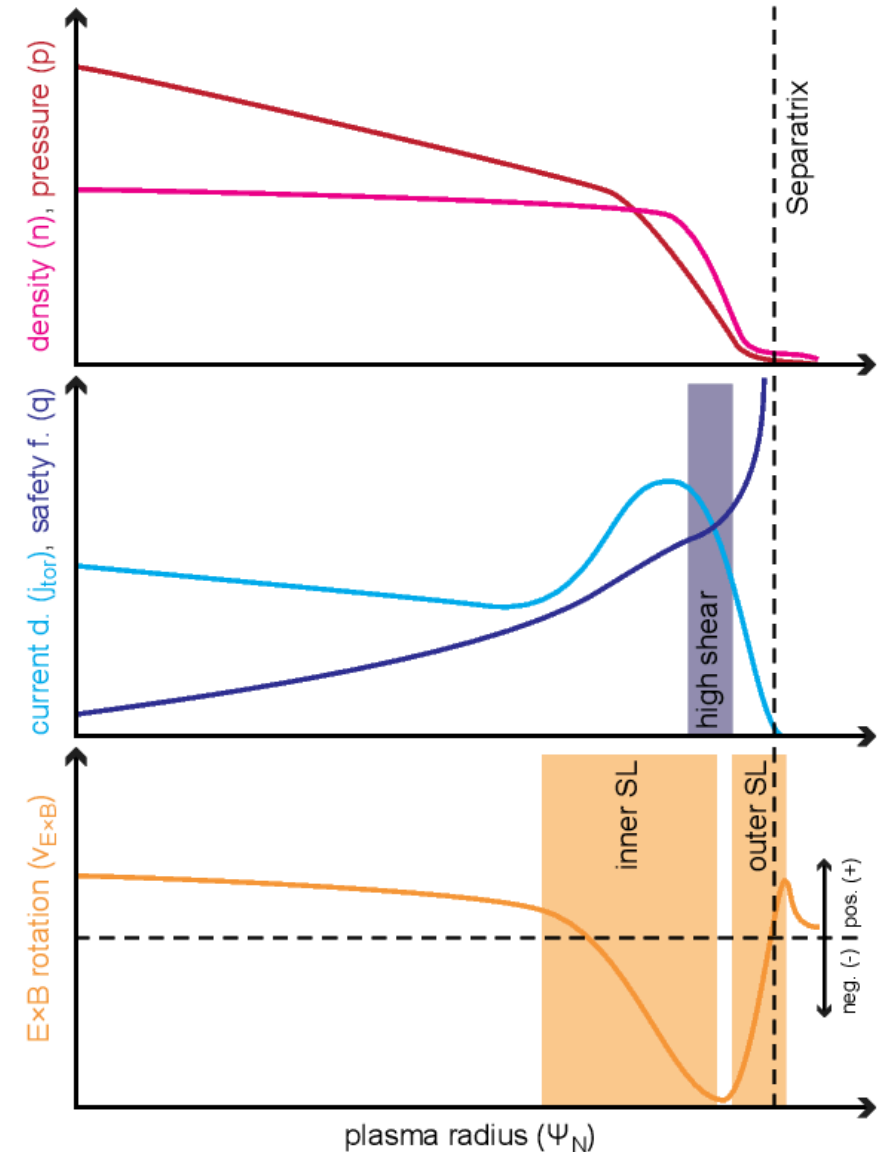
➢ Region of high magnetic shear

- **$E \times B$  rotation ( $v_{E \times B}$ )**

- Radial electric field ( $E_r$ )

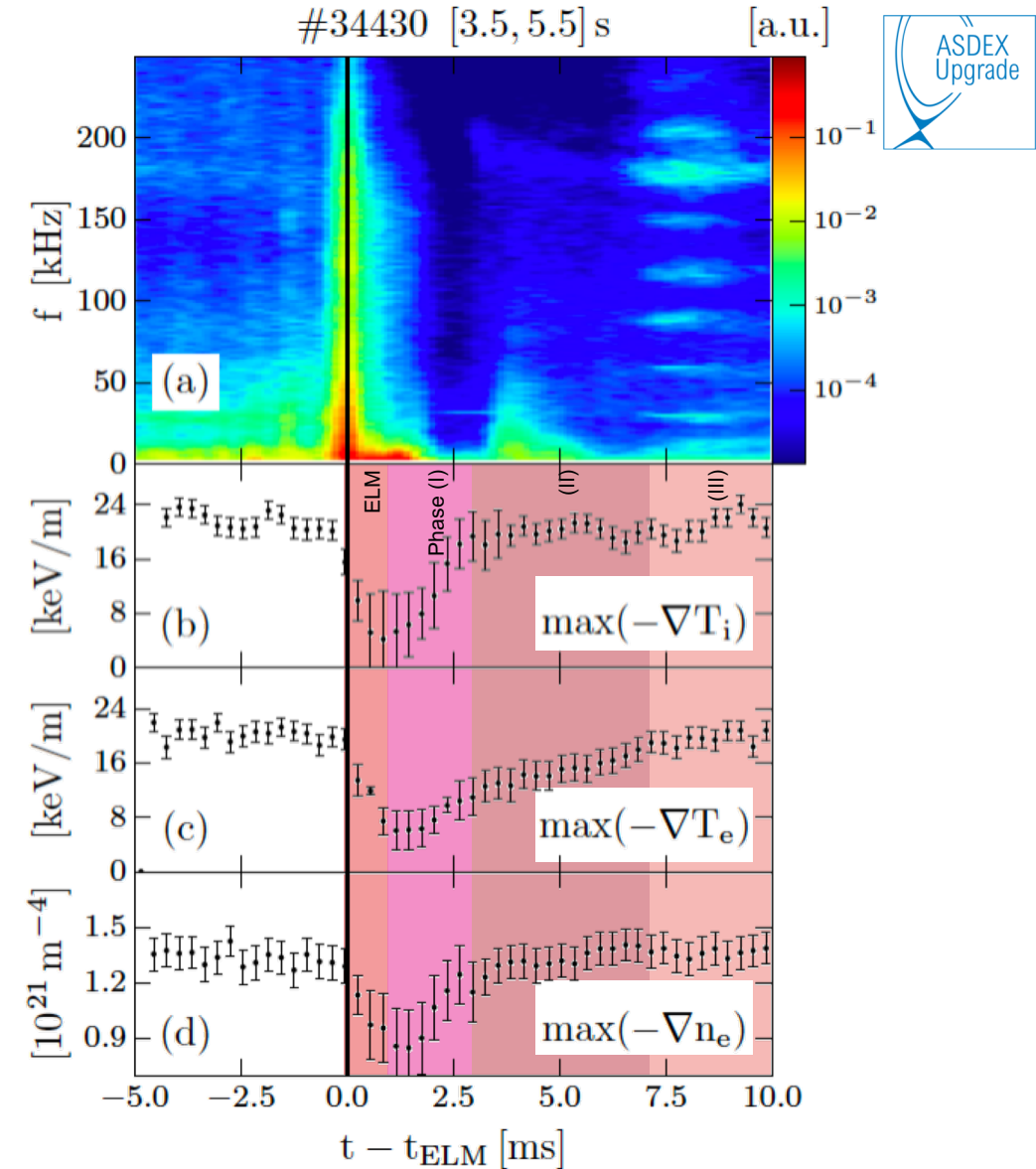
$$E_r = \frac{\nabla p_\alpha}{Z_\alpha e n_\alpha} - v_{\Theta, \alpha} B_\phi + v_{\phi, \alpha} B_\Theta$$

➢ Sheared flows suppress instabilities



# Distinct pedestal recovery phases & fluctuations

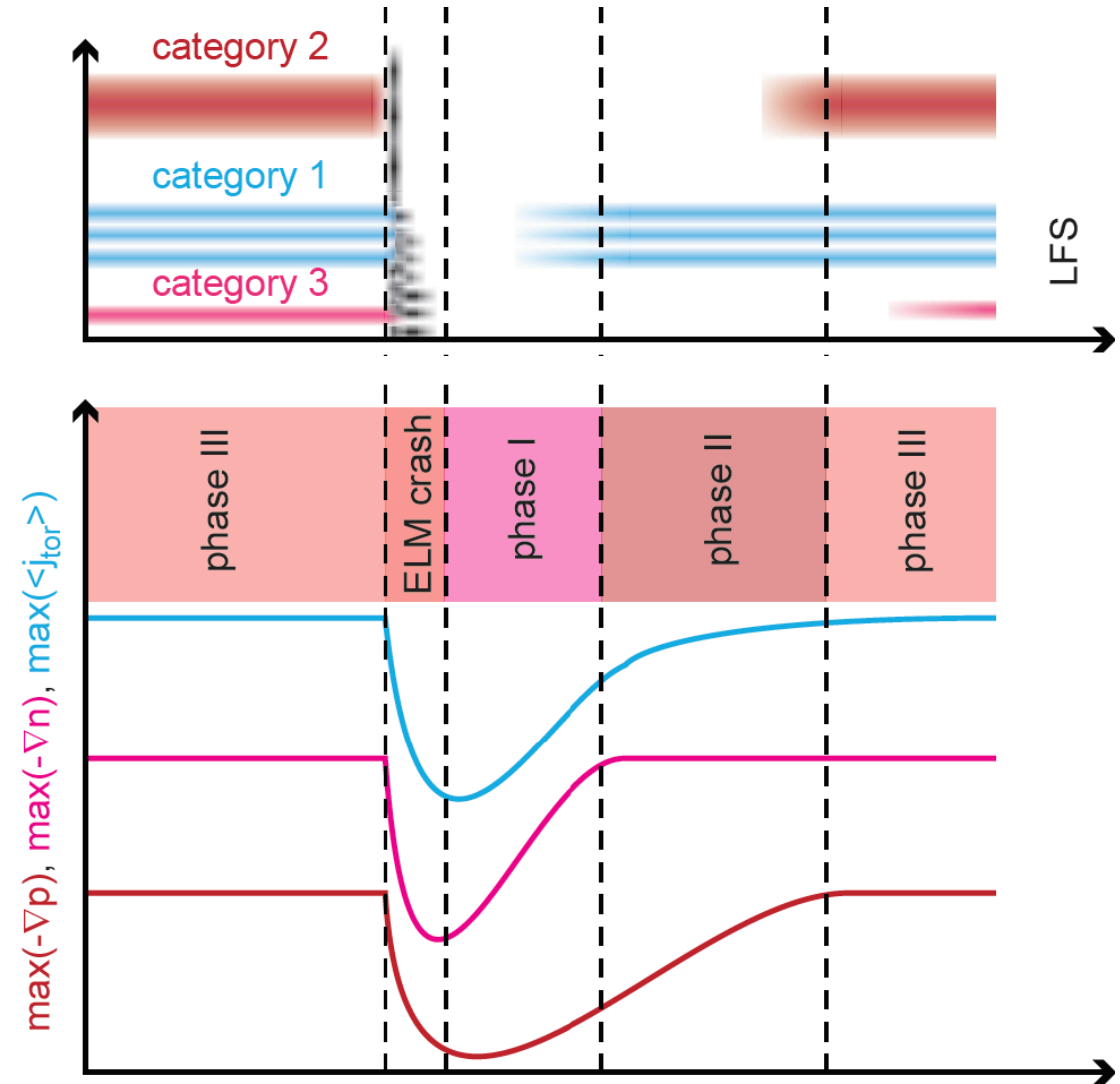
- **Phase (I):**
  - Electron density ( $n_e$ ) gradient and ion Temperature ( $T_i$ ) gradient
    - Fluctuations absent!
- **Phase (II):**
  - Electron temperature ( $T_e$ ) gradient
    - Medium frequency range fluctuations
- **Phase (III):**
  - Gradient saturation
    - High frequency fluctuations
    - Low frequency fluctuations and precursor modes



[M. Cavedon et al., PPCF 2017, PSI 2018 & JNM submitted]

# Abstract picture of the pedestal evolution

- **Phase (I):**
  - Electron density ( $n_e$ ) gradient and ion Temperature ( $T_i$ ) gradient
    - Fluctuations absent!
- **Phase (II):**
  - Electron temperature ( $T_e$ ) gradient
    - Medium frequency range fluctuations
- **Phase (III):**
  - Gradient saturation
    - High frequency fluctuations
    - Low frequency fluctuations and precursor modes





# Three instability categories – An Overview

- **Category 1**

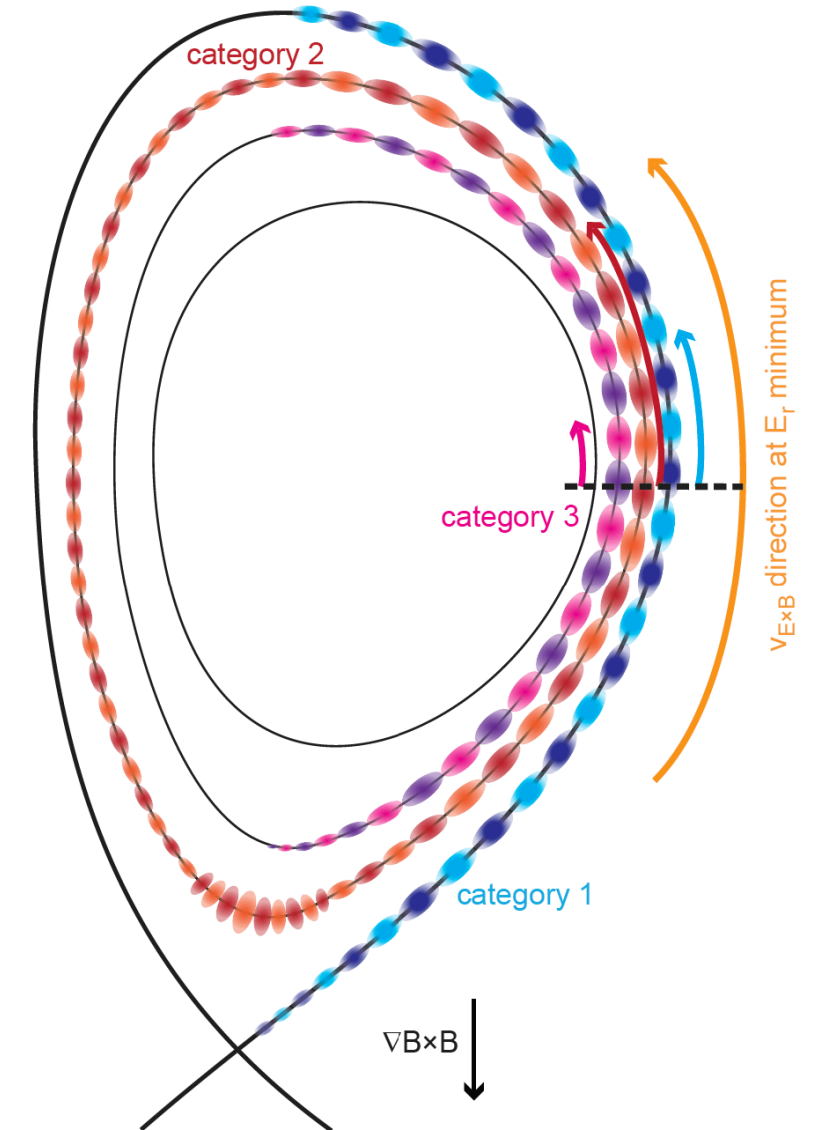
- Separatrix localized
  - Appears at medium frequency range (30 kHz to 150 kHz)
  - Onset after pedestal recovery phase I
  - ‘Ballooned’ mode structure

- **Category 2**

- Localized towards the  $E_{r,min}$ 
  - Appear at high frequency range (> 200 kHz)
  - onset connected to  $T_e$  pedestal evolution (after recovery phase II)
  - HFS magnetic response

- **Category 3**

- Localized at the pedestal top
  - Appear at low frequency range (< 30 kHz)



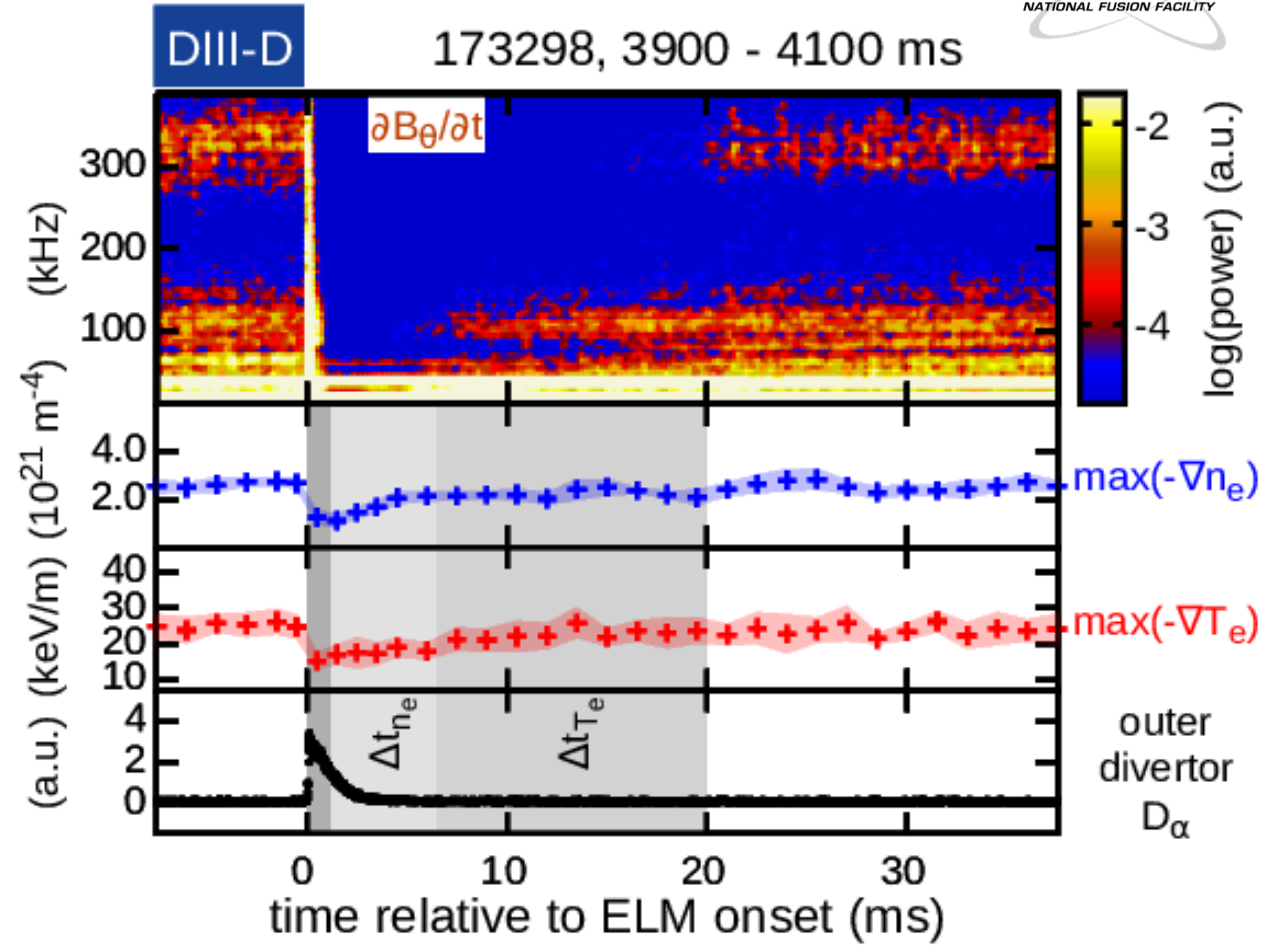
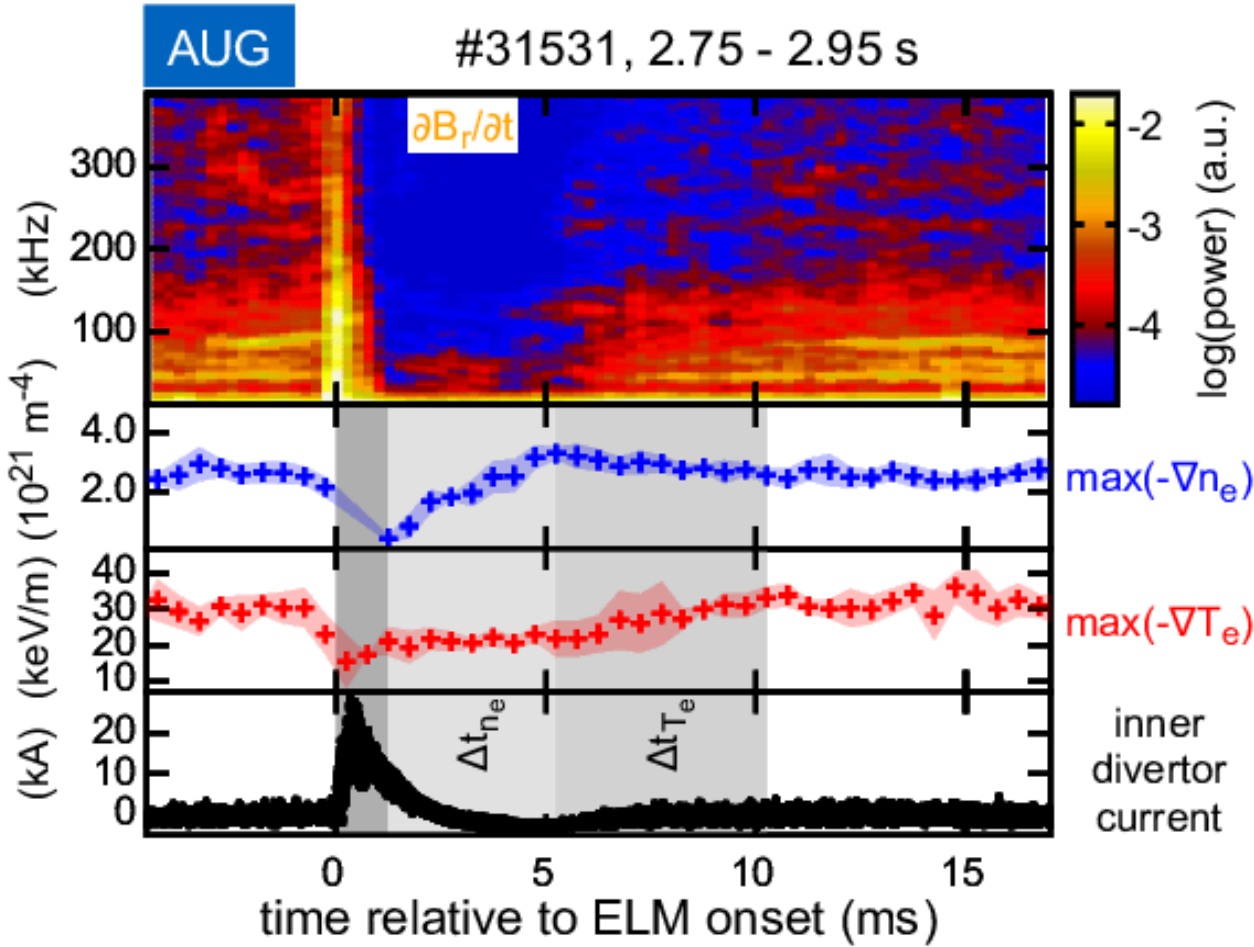
[F. M. Laggner et al., PSI 2018 & JNM submitted]

# Saturated instabilities – Present for tens of ms

Category 1

Category 2

Category 3

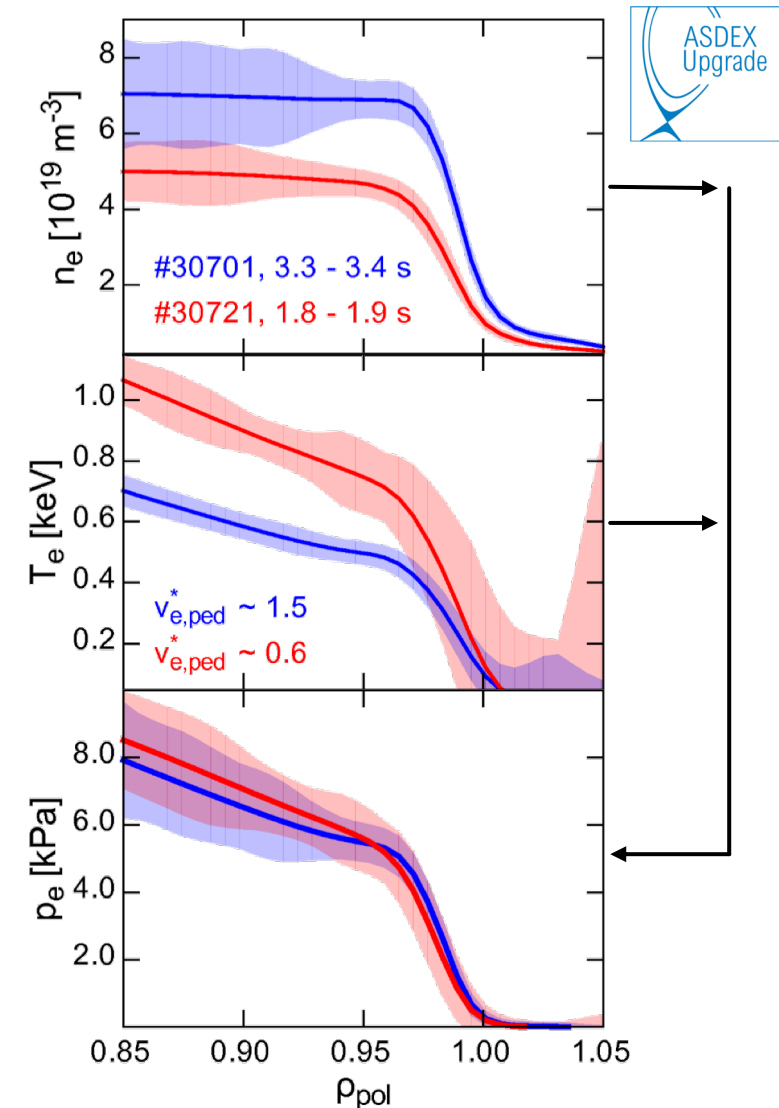


→ Coupling has to occur to get into saturated states

[F. M. Laggner et al., IAEA FEC 2018]

# Test: Collisionality dependence – pressure match

- **High (#30701) and low (#30721) pedestal top electron collisionality  $\nu_{e,ped}^*$**
- **Motivation for comparison:**
  - Pressure (gradient) driven instabilities should not change their behaviour
- **In both discharges gradients are clamped before the ELM onset ('soft limit')**



# Sequence of pedestal recovery phases remains



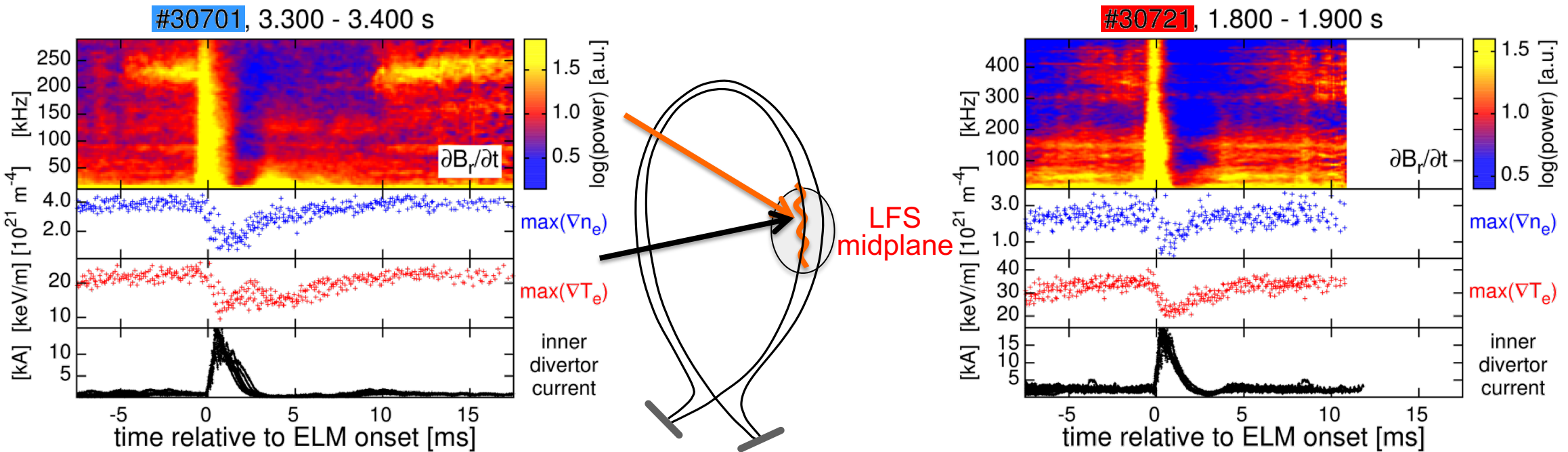
## Category 2

- **First  $n_{e,ped}$  recovery, then  $T_{e,ped}$**
- High frequency fluctuations start afterwards

- $\max(\nabla n_e)$  and  $\max(\nabla T_e)$  clamped when high frequency fluctuations
- Detected fluctuation frequency differs in both cases

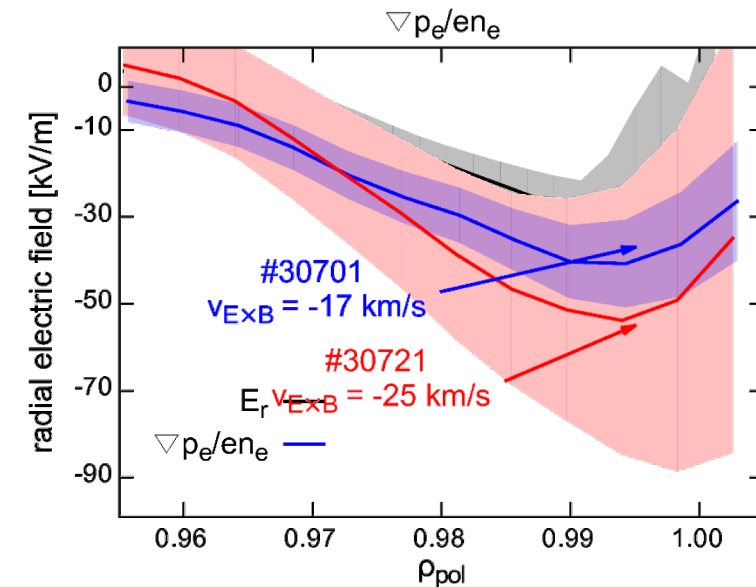
High  $v_{e,ped}^*$  (#30701) case

Low  $v_{e,ped}^*$  (#30721) case



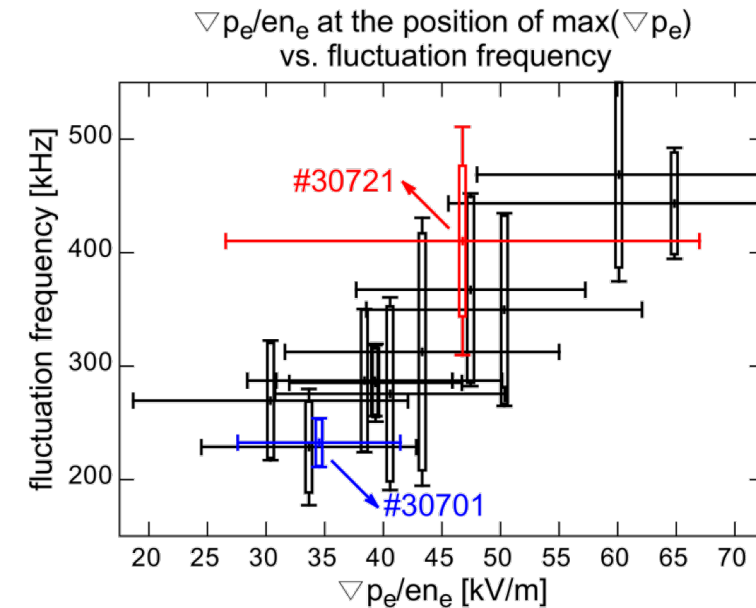
→ What determines the detected fluctuation frequency?

- H-mode → strong  $E \times B$  background velocity at the edge
- ASDEX Upgrade:  $E_r$  is well described by estimation  $\nabla p_i / en_i$  in the steep gradient region  
[E. Viezzer et al., NF 2014]
- $E_r$  and  $\nabla p_e / en_e$  agree within their errors in the analyzed cases



## Category 2

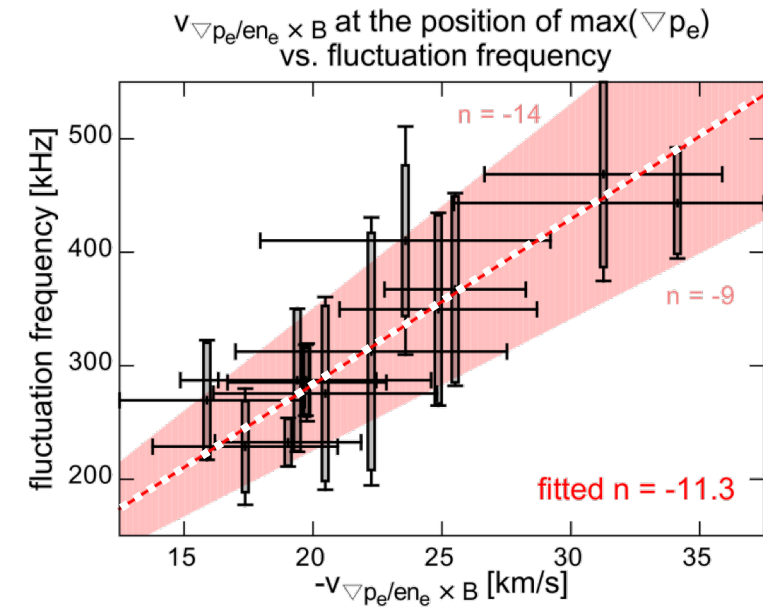
- 11 discharge intervals:
  - Constant  $I_p$  and  $B_t$
  - Selected to span wide range of  $\nabla p_e / n_e$
  - Clear magnetic fluctuations
    - Onset correlated to  $T_{e,ped}$  recovery
- Detected fluctuation frequency increases with  $\nabla p_e / n_e$  at position of  $\max(\nabla p_e)$



➔ Mode is located in the steep gradient region

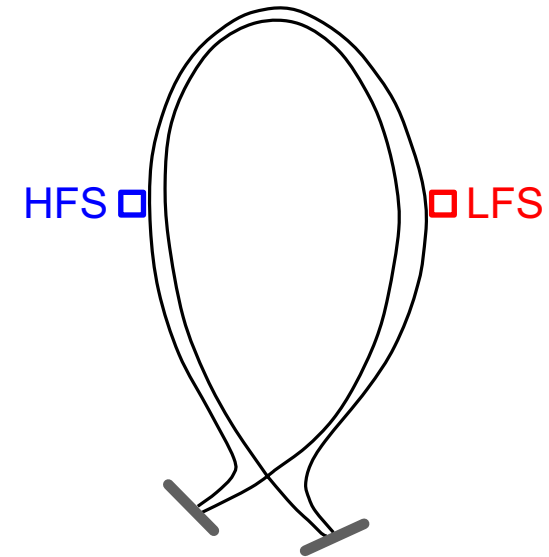
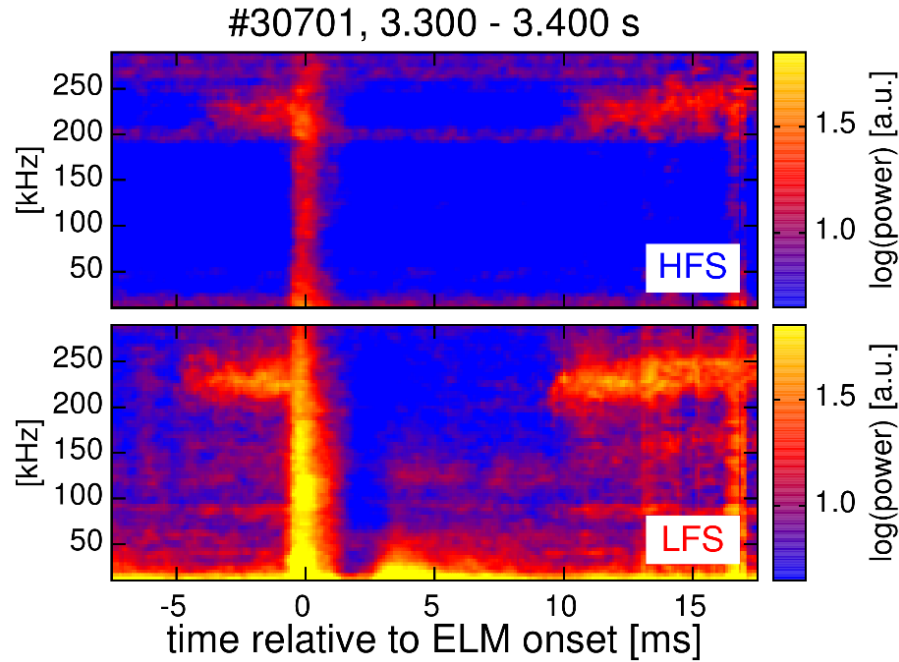
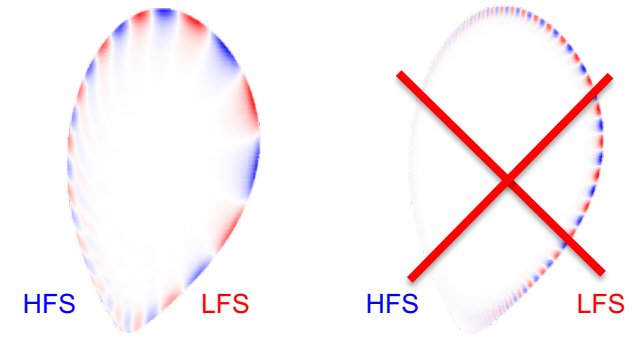
## Category 2

- Fit of  $n$  using the discharge intervals with different  $\nabla p_e / n_e$
- Fit of toroidal mode number:
  - $n \sim U_{\text{tor}} \cdot f_{\text{magn}} / (v_{\nabla p_e / n_e} \cdot q \cdot U_{\text{tor}} / U_{\text{pol}} + v_{\text{tor}})$
- Fitted  $n \sim -11$ 
  - In agreement with  $n$  numbers determined from magnetic pickup coils



## Category 2

- Fluctuation signature visible on the HFS
  - Similar onset as on the LFS
  - Same frequencies as on LFS

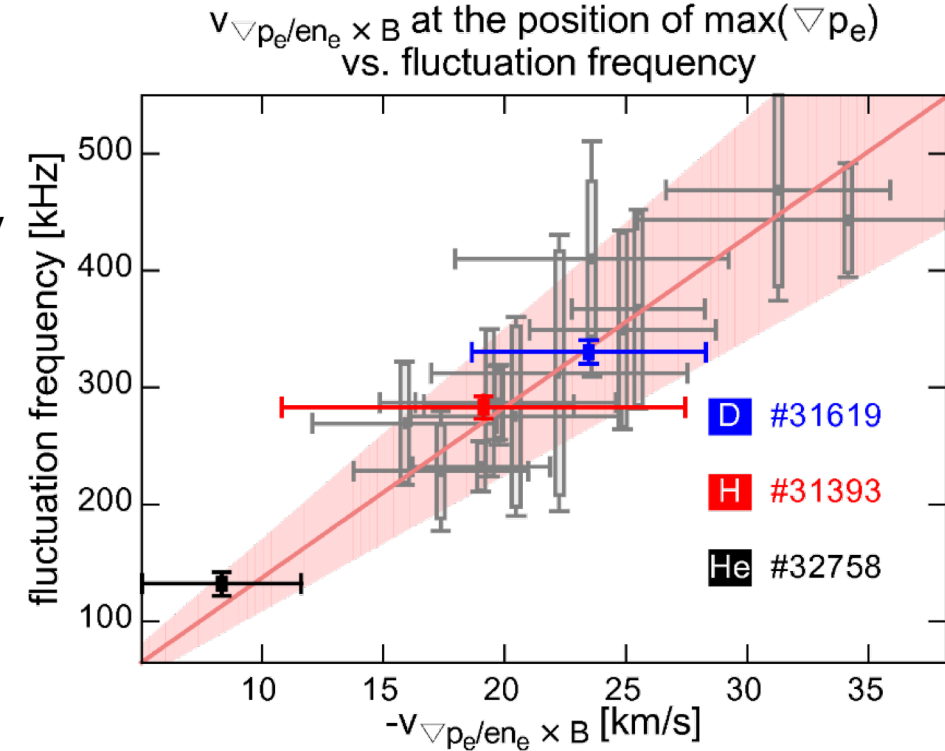
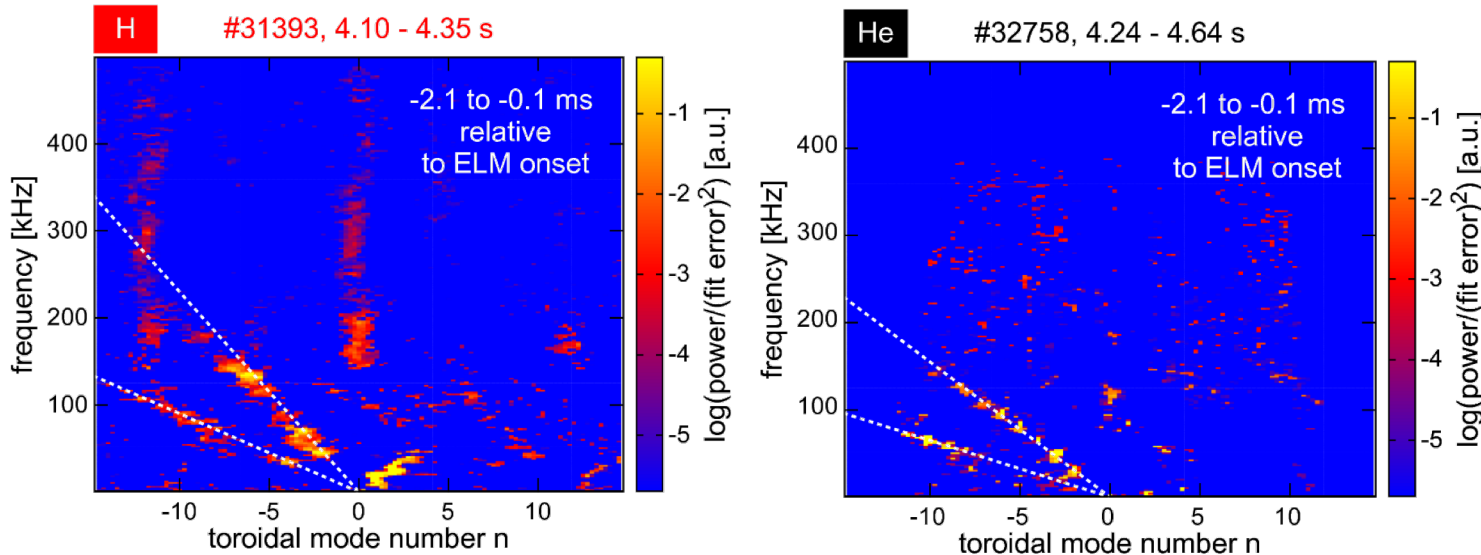


[F. M. Laggner et al., PPCF 2016]



## Category 2

- **Mode propagation with the background  $E \times B$  velocity**
  - Toroidal mode structure with  $n \sim -11$  in all investigated cases
- **Comparison of D, H and He plasmas**
  - Similar sequence of pedestal recovery phases
    - Dominant mechanisms in the pedestal recovery are not changed by a change of the main ion species



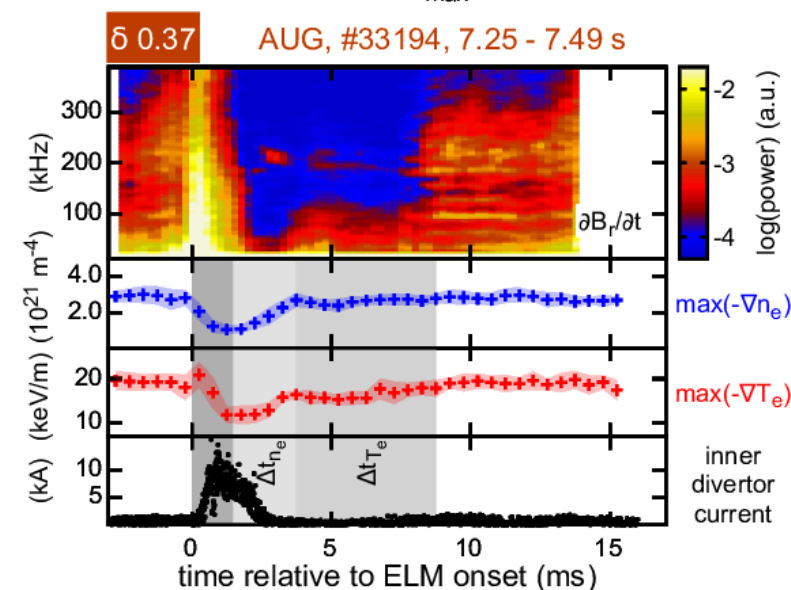
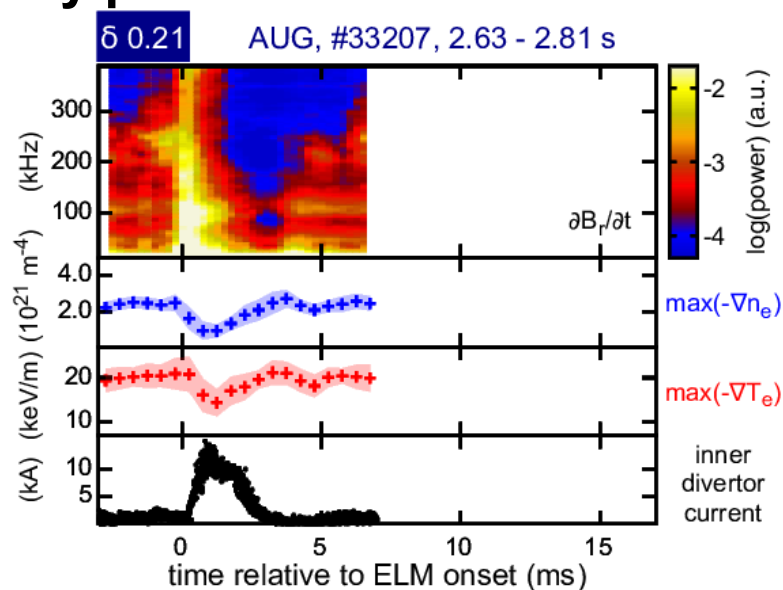
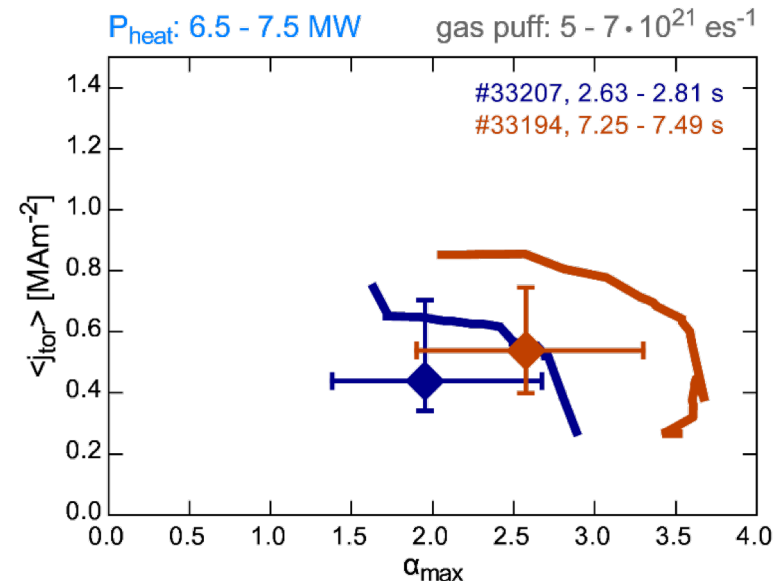
[F. M. Laggner et al., APS invited 2016 & POP 2017]

# Test: Shape dependence – Triangularity variation

Category 1

Category 2

- **ELM frequency ( $f_{ELM}$ ) and PB boundary affected**
  - Reduction of  $f_{ELM}$ 
    - Pedestal recovery phases extended at high triangularity
  - Extension of PB stable area
- **BUT: Sequence of pedestal recovery phases remains**
  - Fluctuation onsets stay correlated

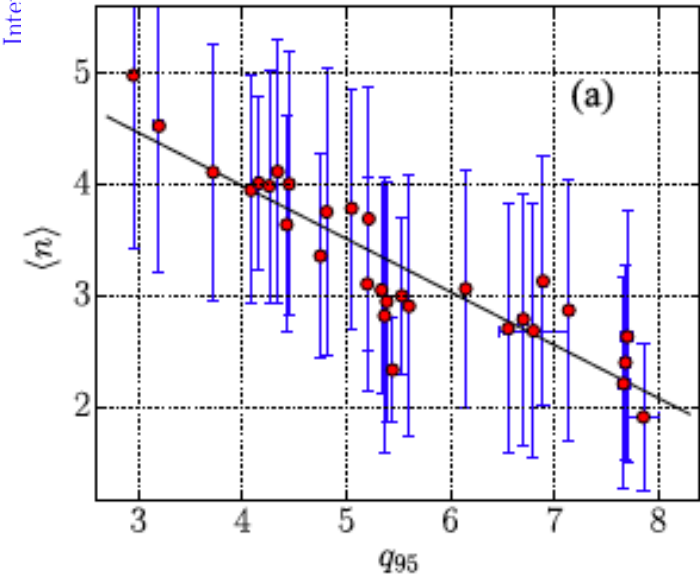
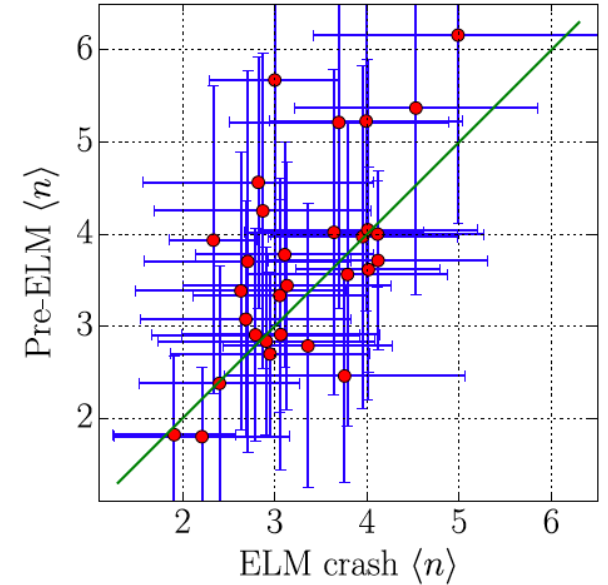
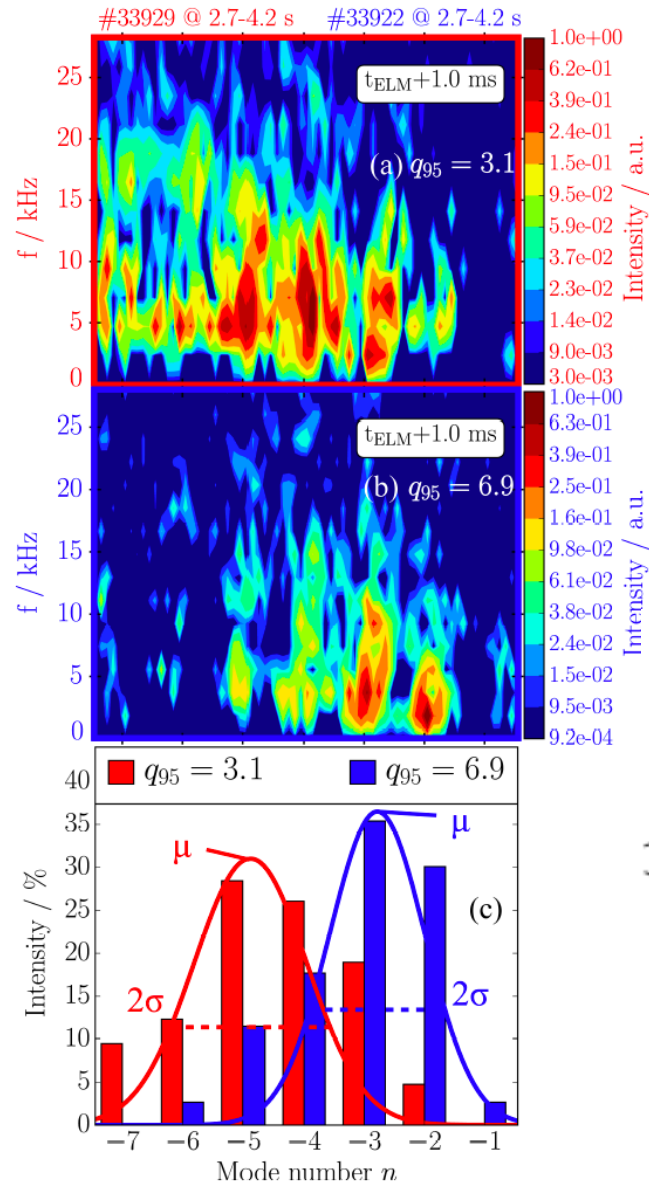


[F. M. Laggner et al., IAEA FEC 2018]

# Test: Safety factor dependence – $I_p$ variation

## Category 1

- Study focused on the structure of the ELM crash
- BUT: pre-ELM and ELM structure are correlated
- Average toroidal mode number  $\langle n \rangle$  decreases with increasing  $q_{95}$ 
  - Poloidal structure conserved



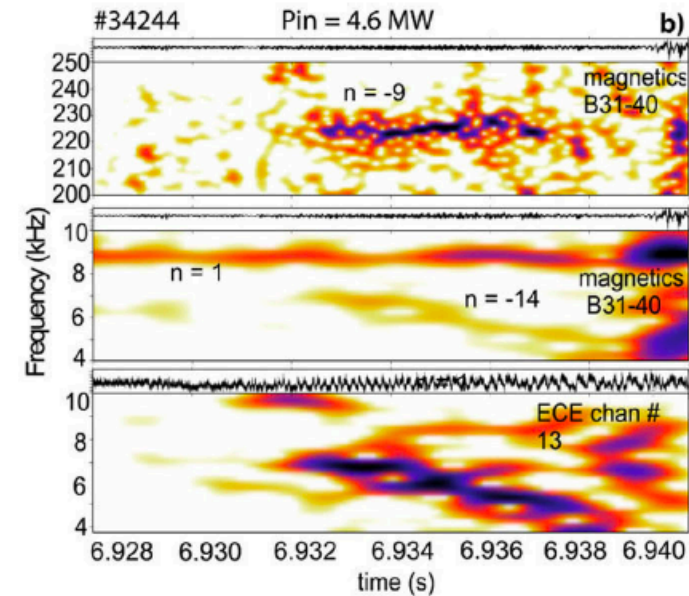
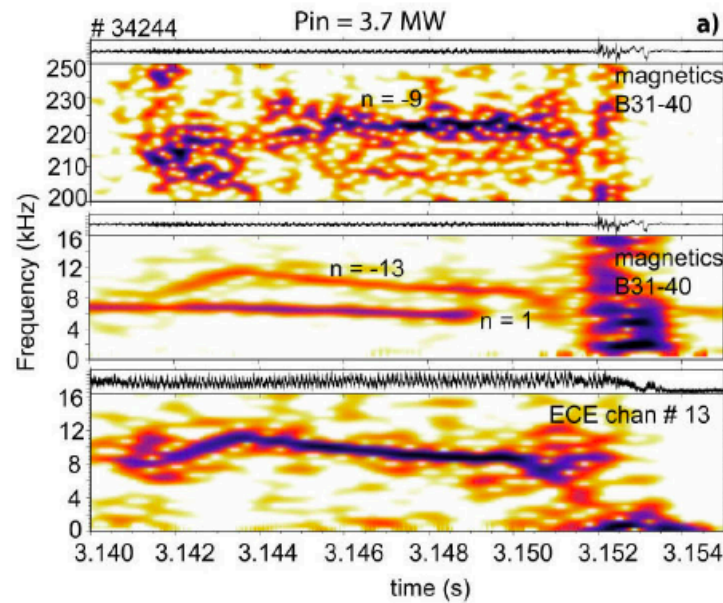
[A. F. Mink, et al., PPCF 2018]

# Category III localized at the pedestal top



Category 3    Category 2

- **Analysis from ECE & magnetics**
  - Category III at low frequency in the ECE & magnetics
  - Category II visible in magnetics
- **Change Category III frequency with  $P_{NBI}$** 
  - Decrease of pedestal top rotation



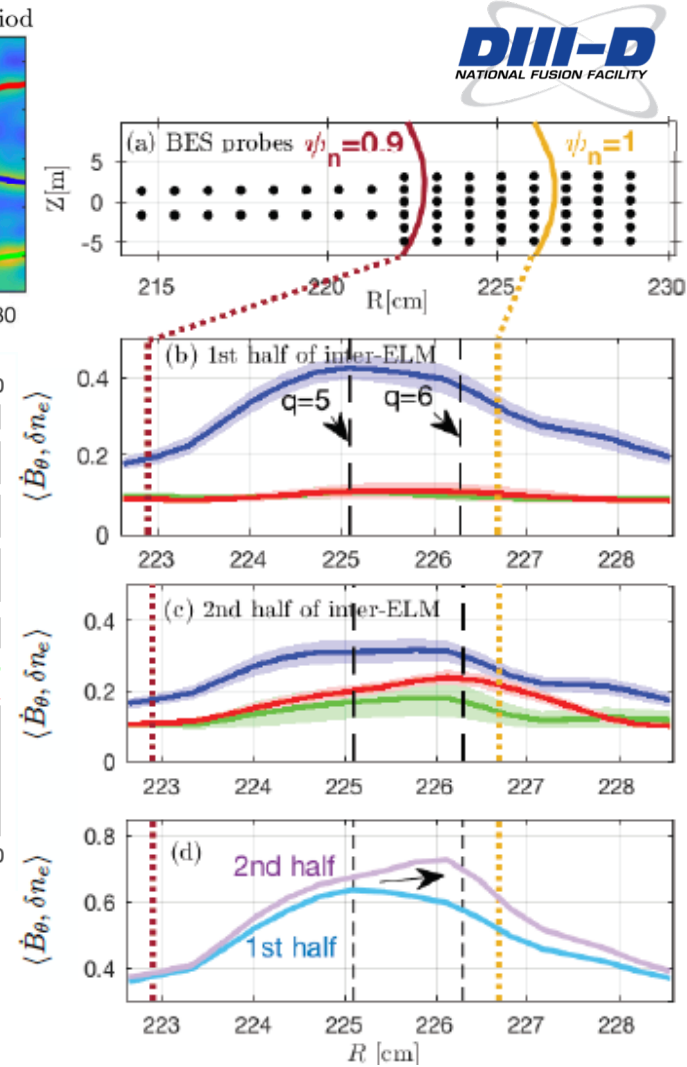
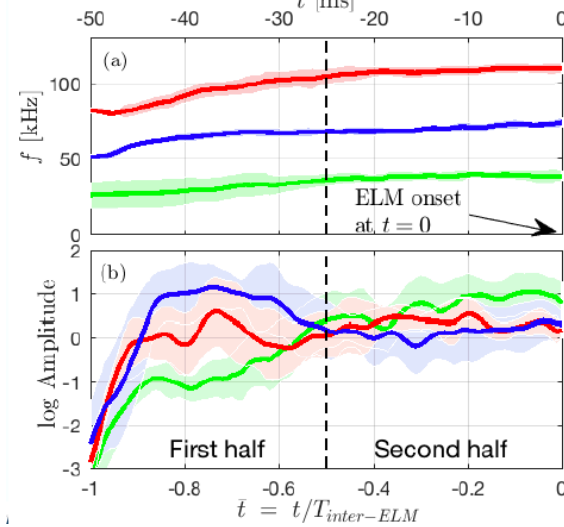
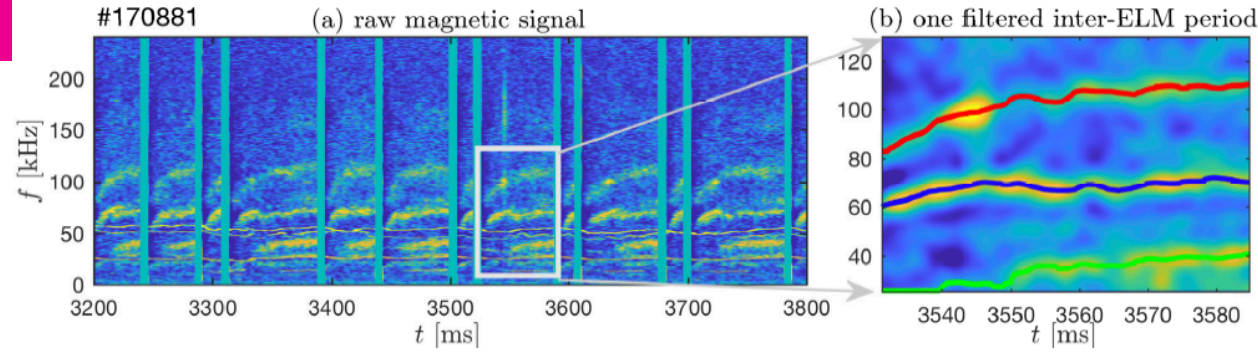
[B. Vanovac, et al., NF 2018]

# Matching condition for Category I and III

Category 1

Category 3

- Suggested to be related to the ELM onset
  - Non-linear coupling of inter-ELM instabilities
- Fluctuation band amplitudes tracked through ELM cycle
  - Change in the spectral power of individual bands
- Radial localization of bands using BES
  - Category III (green) further inwards



[A. Diallo, et al., PRL 2018]

# Summary - Three instability categories

- **Category 1**

- Separatrix localized
  - Appears at medium frequency range (30 kHz to 150 kHz)
  - Onset after pedestal recovery phase I
  - 'Ballooned' mode structure

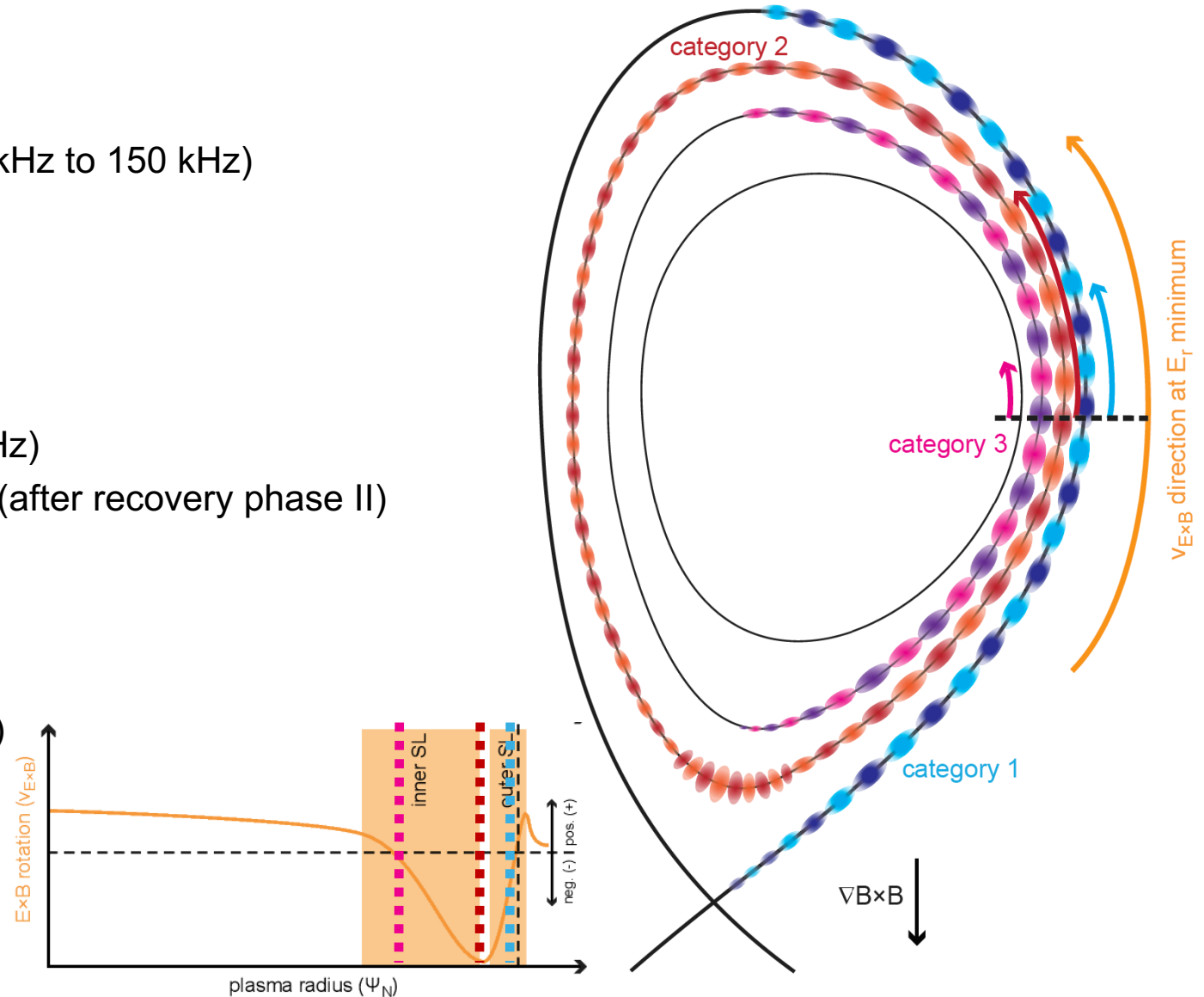
- **Category 2**

- Localized towards the  $E_{r,min}$ 
  - Appear at high frequency range (> 200 kHz)
  - onset connected to  $T_e$  pedestal evolution (after recovery phase II)
  - HFS magnetic response

- **Category 3**

- Localized at the pedestal top
  - Appear at low frequency range (< 30 kHz)

- **MODELLING CHALLENGED TO REPRODUCE 'ROBUST' INSTABILITIES**



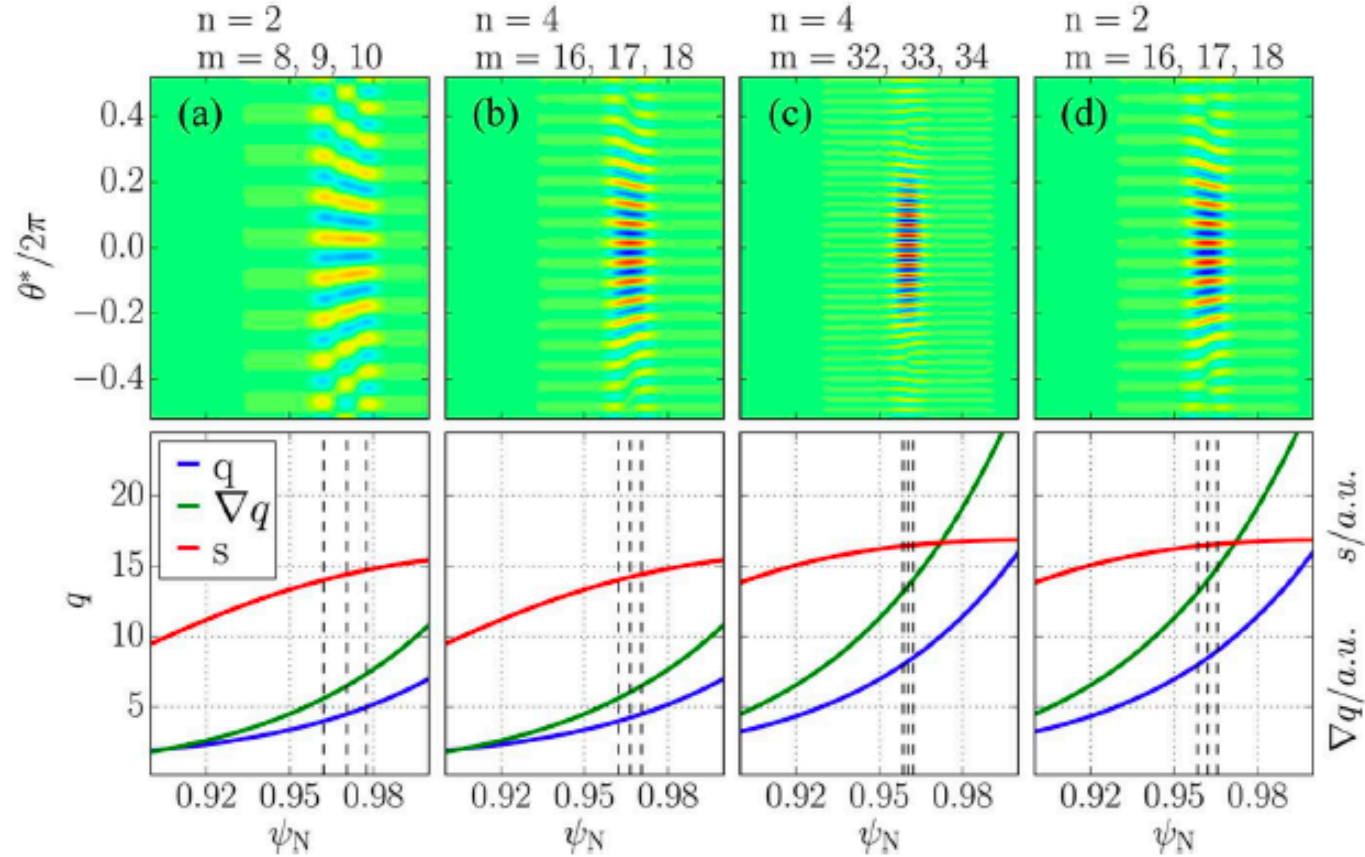
[F. M. Laggner et al., PSI 2018 & JNM submitted]



# Why n changes with $q_{95}$

## Category I

- Minimization of n for a given distance of resonances



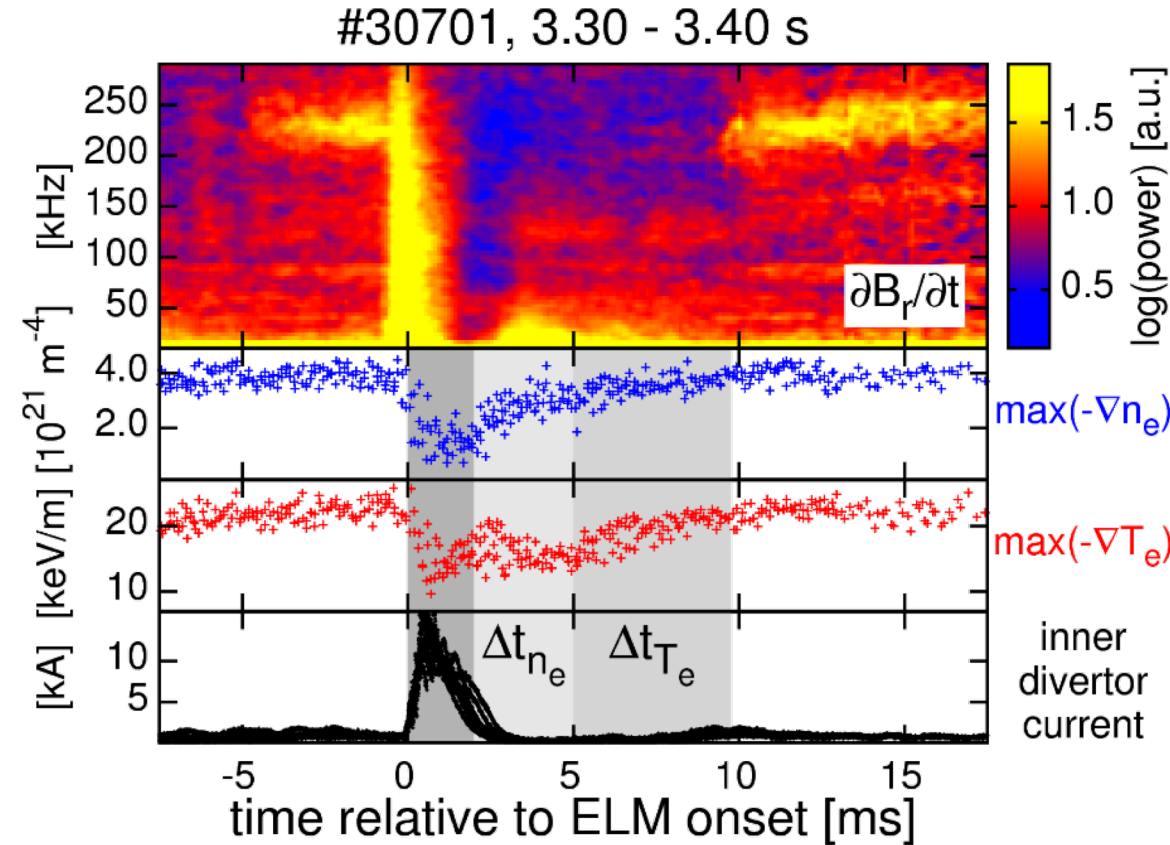
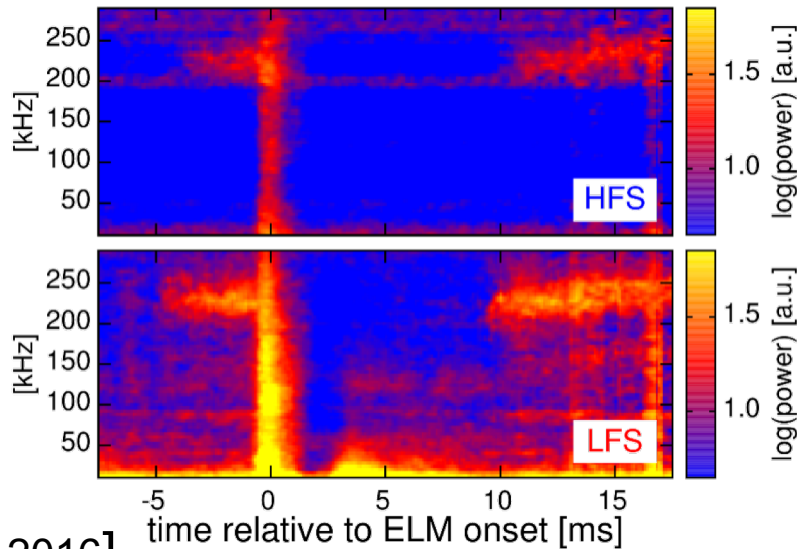
[A. F. Mink, et al., PPCF 2018]



# Inter-ELM pedestal evolution in AUG



- **Distinct recovery phases of  $n_e$  and  $T_e$  profiles**
  - $\max(-\nabla n_e)$  saturates with onset of medium frequency fluctuations
  - $\max(-\nabla T_e)$  evolves till high frequency fluctuation onset
- **Fluctuation signature visible on the HFS**



[F. M. Laggner et al., PPCF 2016]

• Pedestal recovery phases in **D** and **H**

- 1)  $n_e$  pedestal
- 2)  $T_e$  pedestal

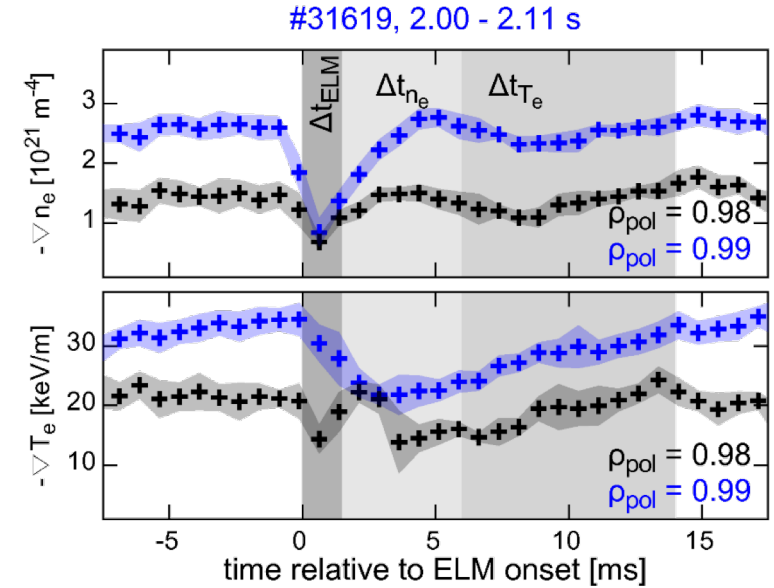
• Different timescales

- attributed to changes in  $P_{net}$ , gas puff and neutral velocity

➤ Indication for similar mechanisms acting in the pedestal recovery

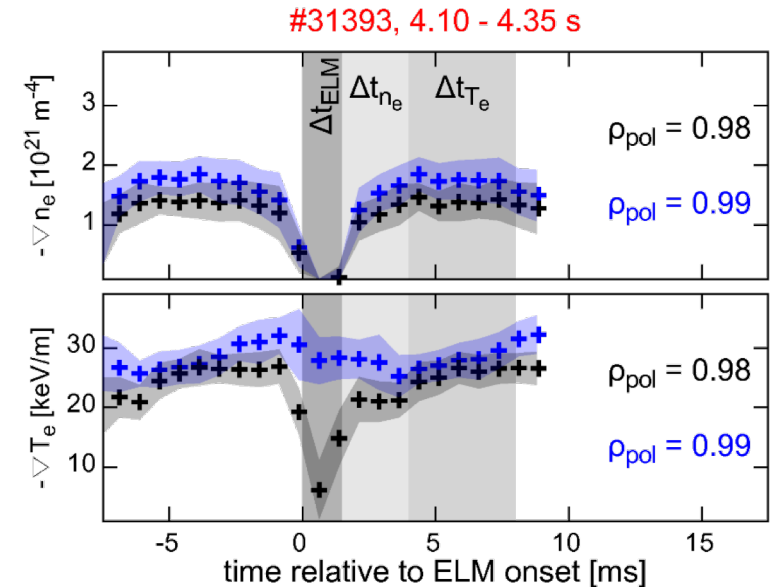
**D**

$P_{net}$   
~ 3.8 MW  
gas puff  
 $1.5 \cdot 10^{21} \text{ s}^{-1}$



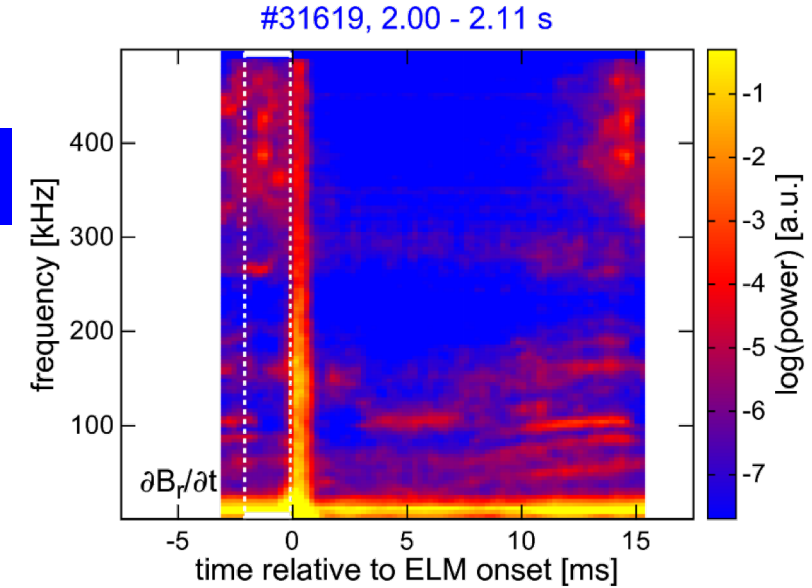
**H**

$P_{net}$   
~ 7.3 MW  
gas puff  
 $12 \cdot 10^{21} \text{ s}^{-1}$

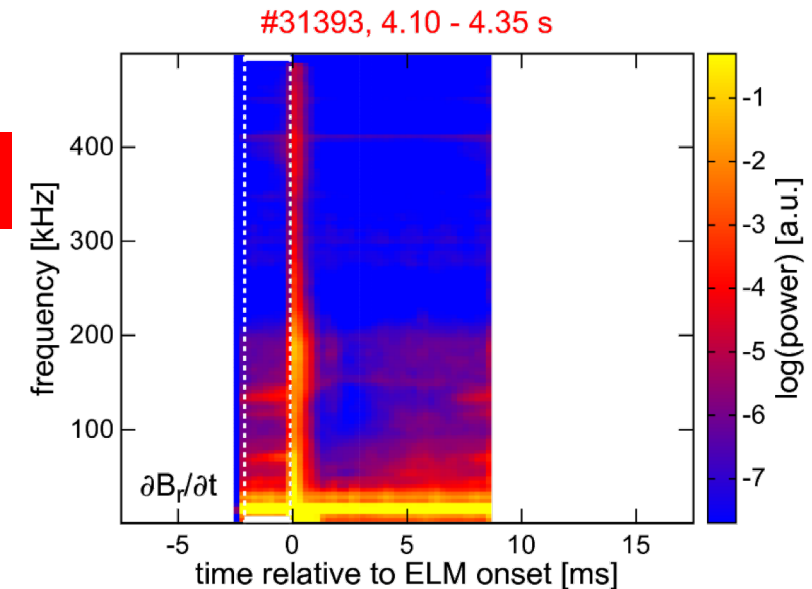


- $\partial B_r / \partial t$  measured at the LFS midplane
  - Radial magnetic fluctuations ( $\partial B_r / \partial t$ )
- Core modes
  - Frequency < 40 kHz
- Lower magnetic activity during  $\Delta t_{ne}$ 
  - 40 kHz < frequency < 200 kHz
- After  $\Delta t_{Te}$  activity at high frequencies
  - Frequency > 200 kHz

D

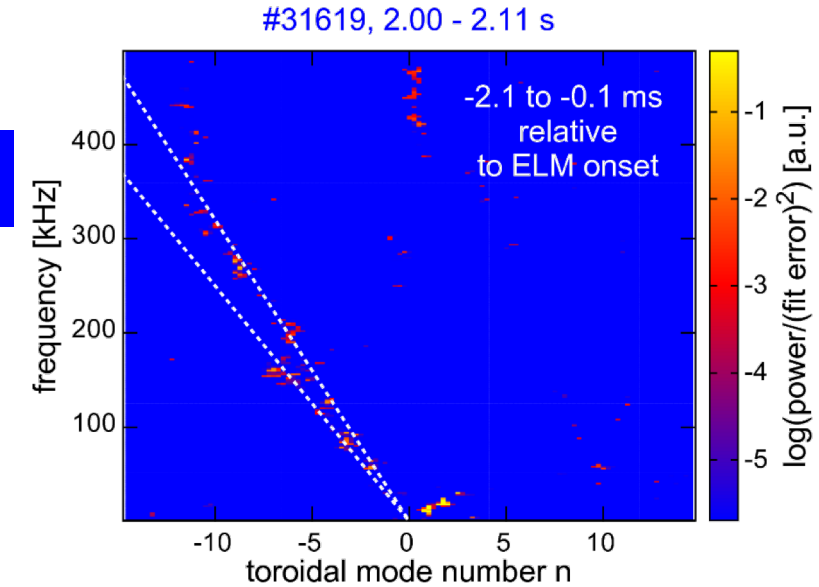


H

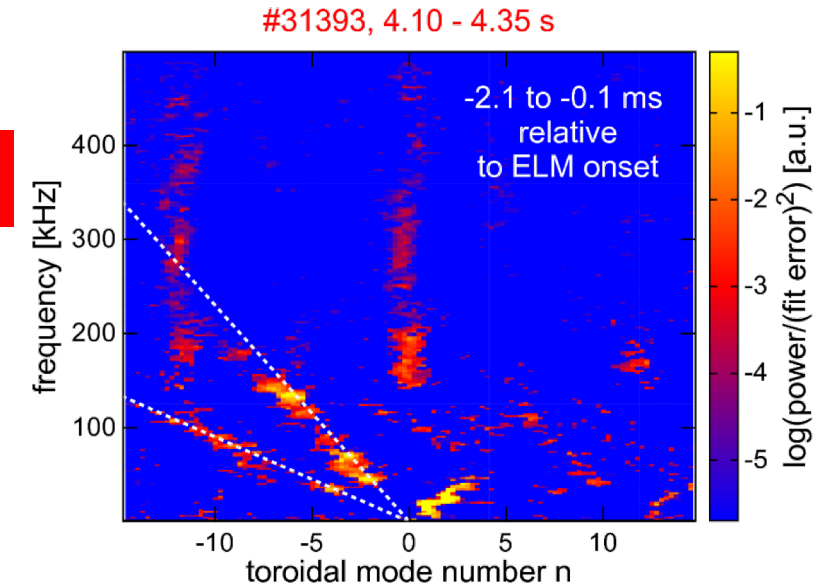


- Negative n:
  - Counter-current propagation or propagation in electron diamagnetic direction
  - Direction of the  $E \times B$  background flow
    - $E_r$  at the edge approximated by  $\nabla p / en$   
[E. Viezzer et al., NF 2014]
- Two mode number branches with similar n  
[F. Mink et al., accepted in PPCF]
- Slope represents different rotation velocity relative to the lab frame
  - $E \times B$  velocity affected by shallower  $\nabla ne$

D

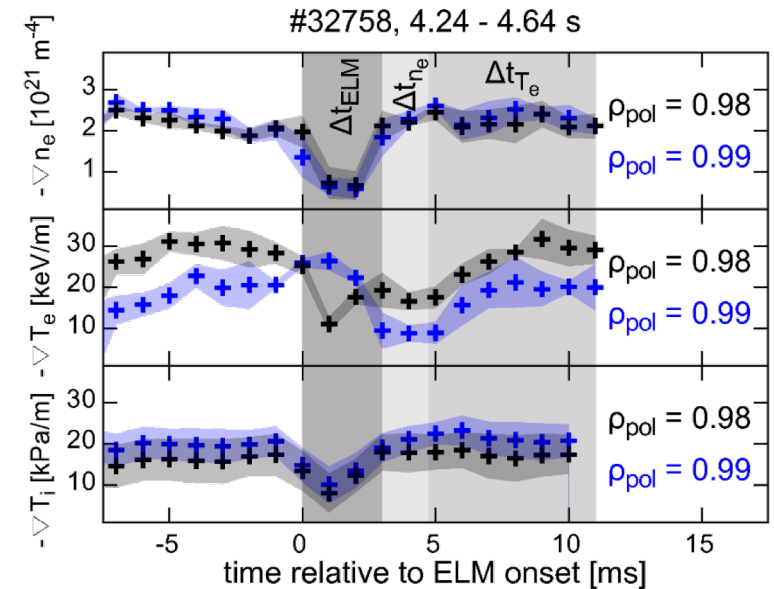


H



- $\nabla T_i$  recovers during  $\Delta t_{ne}$ 
  - Established before the recovery of  $\nabla T_e$
- Consistent with recent findings in **D** plasmas
  - Poster on Friday
    - M. Cavedon et al., Session YP10: YP10.00057  
[M. Cavedon et al., PPCF in preparation]

He



- Lower magnetic activity during  $\Delta t_{ne}$ 
  - 40 kHz < frequency < 200 kHz
- Two mode number branches
- Slope shallower than for **D** and **H**
  - Low rotation velocity relative to the lab frame

He

